

# Ultrashort Pulse Processing of Transparent Ceramics: The Role of Electronic and Thermal Damage Mechanisms

Christian Kalupka<sup>1</sup>, Martin Schmalstieg<sup>2</sup> and Martin Reininghaus<sup>1</sup>

<sup>1</sup> Fraunhofer Institute for Laser Technology ILT, Steinbachstraße 15, 52074 Aachen, Germany  
E-mail: christian.kalupka@ilt.fraunhofer.de

<sup>2</sup> Chair for Laser Technology LLT, RWTH Aachen University, Steinbachstraße 15, 52074 Aachen, Germany

In this study, we investigate the ultrashort pulse processing of the transparent, so-called, spinel ceramic ( $\text{MgAl}_2\text{O}_4$ ). We examine the dominant underlying damage mechanisms by an adjustment of the processing parameters. The applied pulse duration is varied from 2 ps to 80 fs to investigate the impact of the electronic and thermal damage mechanisms on the observed modifications in the material. For surface structuring or ablation cutting conditions, pulse repetition rates below 1 MHz are used leading to electronic damages in form of micro-cracks and spikes inside the volume for pulse durations from 1 ps to 2 ps. By a decrease of the pulse duration to 80 fs, we are able to reduce the electronic damages due to a higher absorption of the laser pulse energy at the spinel surface. By an increase of the pulse repetition rate to 2 MHz, we find evidence for thermal melting of the spinel surface due to the impact of heat accumulation, which leads to a loss of the unique structural properties of the spinel.

DOI: 10.2961/jlmn.2018.02.0012

**Keywords:** ultrashort laser pulses, processing, dielectrics, ceramics, spinel, ablation mechanisms

## 1. Introduction

Due to the recent technical advances, the demands on new materials for markets such as consumer electronics, semi-conductor industry or ballistic protection applications have increased significantly. Therefore, besides the use of conventional amorphous glasses, novel materials like transparent ceramics were developed which exhibit promising potential for many different applications due to their unique mechanical strength, thermal stability, crystal structure and high refractive index [1].

In general, the processing of transparent materials can be achieved by focused ultrashort laser pulses due to non-linear absorption processes for high local intensities even though the material is transparent for the wavelength of the used laser radiation [2,3]. Typically, non-linear multiphoton ionization and tunnel ionization lead to an initial generation of free electrons in the conduction band of the material [4]. The free electrons then gain kinetic energy by the linear absorption of photons due to Inverse Bremsstrahlung absorption. When the kinetic energy of an electron exceeds a critical value, one more electrons can be excited from the valence to the conduction band by impact ionization. The subsequent avalanche ionization leads to a high free electron density, so that the material exhibits quasi-metallic optical properties. Therefore, a strong absorption of the laser radiation is realized, which can lead to strong heating of the lattice and eventually ablation of material due to melting and vaporization. [5]

In dependence on the focusing conditions, several different processes can be realized, for example surface structuring, ablation cutting or generation of highly localized in-volume modifications for selective laser-induced etching [6,7]. Due to the complex superposition of linear and non-linear absorption, interaction and propagation effects like

self-focusing and plasma defocusing for the use of the necessary high intensities, an improved understanding of the impact of the different processing parameters on the underlying ablation mechanisms and therefore resulting material modifications is crucial for an improvement and upscaling of the modification process of transparent materials. Experimental analysis of the energy deposition in amorphous glasses by time-resolved pump-probe microscopy reveal that in particular the pulse duration has a major impact on the amount and spatial distribution of deposited energy [8,9]. In accordance with spatial- and temporal resolved simulations of the energy deposition, the absorbed energy increases significantly for the use of pulse durations in the picosecond (ps) regime compared to the femtosecond (fs) regime [10]. Moreover, for multi-pulse ablation incubation and accumulation lead to a change in energy deposition of subsequent laser pulses. Therefore besides the role of laser pulse parameters like the pulse duration, fluence and pulse overlap, the local energy deposition is also influenced by the pulse-plasma interaction, which can be controlled by the spatial pulse overlap as well as the time between two subsequent pulses which is directly correlated to the pulse repetition rate.

The transparent ceramics used in this study are, so-called, spinel ( $\text{MgAl}_2\text{O}_4$ ). Spinel exhibits several extraordinary properties compared to conventional glasses. For example a high refractive index  $n = 1,72$  at 600 nm, cubic crystal structure, hardness 1464HV10, Young's modulus 274 GPa, high melting temperature 2440 K and a high heat conductivity  $15 \text{ Wm}^{-1}\text{K}^{-1}$  [11]. Thus, the interaction of ultrashort pulsed laser radiation and the spinel might exhibit novel features. Moreover, for the development of a laser-based process of large scale processing of transparent ce-

amics, the underlying ablation mechanisms must be understood.

Therefore, in this study for machining transparent spinel with ultrashort laser pulses, we identify the underlying modification mechanisms and their dependency on the processing parameters. On the one hand side, we analyze the role of incubation on the material modification by the use of a spatial and temporal pulse overlap in such a way, that the heated material relaxes completely after each pulse. This is referred to as electronic damage mechanism, because the excited free electron plasma can be directly correlated with the resulting modification [12]. Moreover, the impact of the pulse duration on the resulting modification and therefore the spatial energy deposition is investigated. On the other hand side, we increase the spatial pulse overlap and decrease the time between subsequent pulses by the application of high pulse repetition rates to investigate the role of heat accumulation on the resulting modification. In the following, this is referred to as thermal damage mechanism. The detailed characterization of the processed areas like surface roughness, damage morphology etc. allows for an estimation of the dominant damage mechanism in dependency on the applied pulse parameters.

## 2. Experimental setup

We use a high power laser source (“Amphos 400”), which emits linear polarized pulses with a central wavelength of 1030 nm, a pulse duration of  $\tau = 2$  ps, a maximum pulse energy of  $E_p = 1$  mJ and an adjustable pulse repetition rate from  $f_{rep} = 0.2$  to 54 MHz. To carry out ablation experiments, we focus the laser radiation onto the surface of the spinel with an f-theta objective with a focal length of 163 mm, resulting in a focal diameter of approximately  $2w_0 = 55$   $\mu\text{m}$ . The laser radiation on the surface is moved by a galvanometer scanner with scanning velocity  $v$  up to 6 m/s. To manufacture cavities, the laser radiation is moved linearly in lines whereas the line separation distance is equal to the pulse overlap PO in scanning direction. The latter is calculated by  $PO = 1 - v/(f_{rep} 2w_0)$ . Additionally, the number of scanned lines  $N$  is chosen between  $N = 1$  and 200.

To perform ablation experiments with a variation of the

pulse duration, we use a chirped pulse amplification Ti:Sapphire laser source which emits pulses with central wavelength of 800 nm and a maximum pulse energy of  $E_p = 2$  mJ. The pulse duration can be set between  $\tau = 80$  fs and 10 ps. The maximum pulse repetition rate is  $f_{rep} = 1$  kHz, therefore the scanning velocity is decreased significantly to provide comparable spatial pulse overlaps. The laser radiation is focused by a plano-convex lens with a focal length of 150 mm resulting in a focal spot diameter of  $2w_0 = 32$   $\mu\text{m}$ .

The used spinel is  $\text{MgAl}_2\text{O}_4$  and was developed by the Fraunhofer Institute for Ceramic Technologies and Systems (IKTS) in Dresden, Germany. The spinel has an average grain size of approximately 0.57  $\mu\text{m}$ , a cubic crystal structure and high homogeneity as well as purity leading to high transparency for high surface qualities. To remove residuals from the sintering and to achieve a flat surface, the spinel was grinded mechanically with a SiC grinding disc resulting in a surface roughness of approximately  $R_a = 3$   $\mu\text{m}$ .

## 3. Results and discussion

In the following, the results are presented and discussed in two sections. In the first section, the results for an electronic damage mechanism are shown by the resulting surface morphology as well as in-volume modifications for the use of low pulse repetition rates. In the second section we investigate the role of heat accumulation and therefore the role of thermal damage mechanism on the processing of spinel by a discussion of the processing results for an increased pulse repetition rate, which leads to a significant spatial pulse overlap and a decreased time between subsequent pulses.

### 3.1 Electronic damage mechanism: Incubation

Cavities with a size of  $1.5 \times 1.5$   $\text{mm}^2$  are manufactured on the surface of the spinel with a mean fluence of  $F = E_p/(\pi w_0^2) = 2$   $\text{J}/\text{cm}^2$  and  $N = 10$  repetitions of scanned layers. To avoid heat accumulation, the peak fluence  $F_{peak} = 2F$  is chosen close to the single pulse ablation threshold of  $F_{thr} = 3.9 \pm 0.1$   $\text{J}/\text{cm}^2$ , which has been estimated by ablation experiments with the method by Liu by

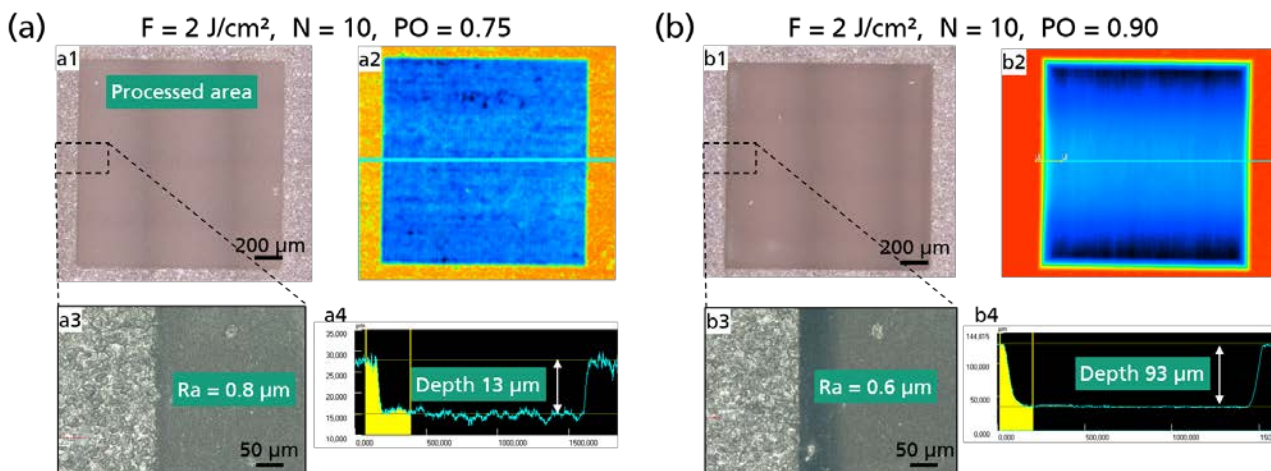


Fig. 1: Manufactured cavities on the surface of spinel with  $f_{rep} = 200$  kHz,  $F = 2$   $\text{J}/\text{cm}^2$ ,  $N = 10$  for different spatial pulse overlaps. (a)  $PO = 0.75$ ; (b)  $PO = 0.90$ . For each pulse overlap, bright field microscopy images of the processed surface are shown as well as measured height profile in a color map and a height profile of the central cross section of each cavity.

measurements of the ablation crater diameter for a variation of the applied pulse energy and a logarithmic fit of the acquired data (not shown here) [13]. Moreover, the pulse repetition rate is set to  $f_{\text{Rep}} = 200$  kHz. In Figure 1 the resulting cavities are shown for two different spatial pulse overlaps  $\text{PO} = 0.75$  and  $0.90$ , respectively. For each pulse overlap, a bright field microscope image of the cavity, a magnified image of the edge of the cavity as well as a height profile of the cavity in a color scale and a one dimensional height profile for the center of the cavity are shown. The height profiles are measured by laser scanning microscopy.

For a pulse overlap  $\text{PO} = 0.75$  the morphology of the processed area is homogenous (Figure 1 (a1)). A comparison of the unmodified and the ablated material in the detailed image of the edge of the cavity shows that the processed area appears darker (Figure 1 (a3)). Moreover, the surface seems smoother compared to the unmodified material. Therefore, the height has been measured (Figure 1 (a2) and (a4)). The depth of the cavity is approximately  $13 \mu\text{m}$ . The surface roughness is measured at different positions in the processed area and is evaluated to approximately  $R_a = 0.8 \pm 0.2 \mu\text{m}$ . Therefore, a decreased of the surface roughness compared to the unprocessed spinel  $R_a = 3 \mu\text{m}$  is achieved. In the next step, we increase the spatial pulse overlap to  $\text{PO} = 0.90$ , while the applied fluence  $F$  and number of scanned layers  $N$  remain constant. The results are shown in Figure 1 (b). The processed area for  $\text{PO} = 0.90$  appears unchanged compared to  $\text{PO} = 0.75$  with regard to the bright field microscope analysis in (b1) and (b3). The height profile (b2) reveals that the ablation depth has increased by approximately a factor 7 to  $93 \mu\text{m}$  compared to  $\text{PO} = 0.75$ . Moreover, at the top and bottom area of the cavity, the ablation depth is increased which can be explained by reflection of the laser radiation at the edge of the cavity, therefore leading to a change of local intensity in regions near the edge of the cavity. The surface roughness of the processed area is estimated to  $R_a = 0.6 \pm 0.2 \mu\text{m}$  therefore remains constant with regard to  $\text{PO} = 0.75$ . Thus we conclude, that for the applied processing parameters heat accumulation is negligible for the ablation process and the ablation is dominated realized by direct vaporization of

the spinel. In the next step to investigate the role of electron damage mechanisms for the spinel, we analyze the material modification inside the volume.

In Figure 2, bright field microscopy images of mechanically polished cross sections of the cavities from Figure 1 are shown. For  $\text{PO} = 0.75$  and  $0.90$ , we observe dark stripes below the processed area, which are orientated perpendicular to the surface. They extend up to approximately  $50 \mu\text{m}$  inside the volume of the spinel (Figure 2 (a1)). For  $\text{PO} = 0.75$ , one dark stripe extends to approximately  $101 \mu\text{m}$  at the edge of the processed area (Figure 2 (a2)). For an increase of spatial pulse overlap  $\text{PO} = 0.90$ , two sharp cracks at both edges of the cavity are observed (Figure 2 (b1)), that extend up to  $78 \mu\text{m}$  inside the volume of the spinel (Figure 2 (b2)). Comparable observations of cracks with lengths up to several  $10 \mu\text{m}$  starting at the edge of an ablation crater are reported in [12] for glass. Numerical simulations as well as recent experimental analysis of the energy deposition inside a glass volume reveal that the cracks originate from local absorption maxima which result from refraction and interference of the laser radiation by the shape of the surface of the ablation crater [6,12]. Accordingly, for an increase of number of pulses per area the cracks become more pronounced due to the high amount of energy deposited in the local absorption maxima which is consistent with the occurrence of cracks for a high spatial pulse overlap  $\text{PO} = 0.90$  in our study.

The energy deposition inside the volume is directly correlated to the applied pulse duration of the ultrashort laser pulses [9,10]. For fs pulse durations and high intensities, the energy is primarily deposited in a small volume located at the surface whereas for ps pulse durations energy can penetrate deeper into the volume due to the decreased peak intensity and longer spatial extend of the pulse. Therefore, in the next step the dependency of the cracks inside the volume of spinel on the applied pulse duration is analyzed. For this, one dimensional ablation lines are manufactured with the Ti:Sapphire laser source for two different pulse durations  $\tau = 80$  fs and  $1$  ps and for each pulse duration different number of scanned lines  $N = 50, 100$  and  $200$ , respectively. The fluence  $F = 5.4 \text{ J/cm}^2$  is kept constant.

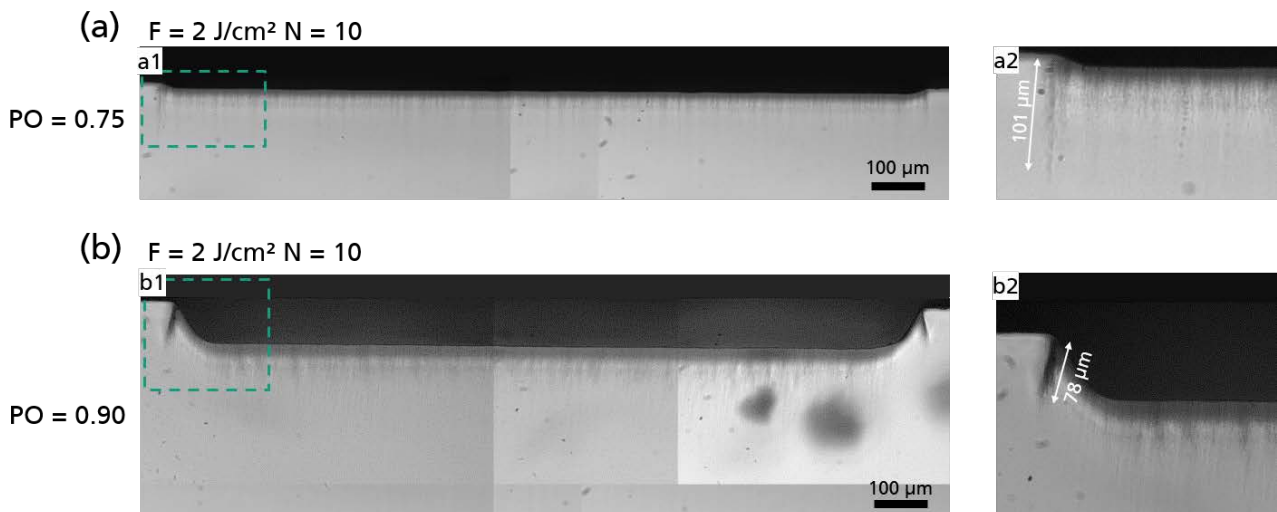


Fig. 2: Bright field microscopy of cross sections of manufactured cavities on the surface of spinel with  $f_{\text{Rep}} = 200$  kHz,  $F = 2 \text{ J/cm}^2$ ,  $N = 10$  for different spatial pulse overlaps. (a)  $\text{PO} = 0.75$ ; (b)  $\text{PO} = 0.90$ .

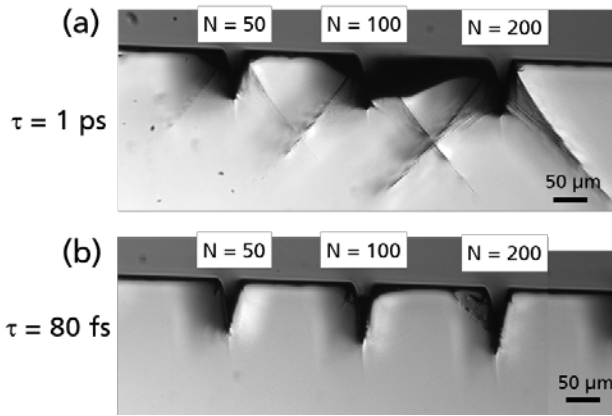


Fig. 3: Bright field microscopy of cross sections of manufactured lines on the surface of spinel with  $f_{rep} = 1$  kHz,  $F = 5.4$  J/cm<sup>2</sup> in dependency on the applied pulse duration  $\tau$  and number of scanned layers. (a)  $\tau = 1$  ps; (b)  $\tau = 80$  fs.

The polished cross sections for all processing parameters are shown in Figure 3.

For a pulse duration  $\tau = 1$  ps, the same features for the cracks in the volume of the spinel are observed compared to the manufactured cavities from Figure 2. In addition, for an increase of number of scanned lines  $N$ , the cracks appear clearer. The long cracks extend several 100  $\mu\text{m}$  inside the volume hence are much longer compared to the cavities due to the higher applied fluence. For a decrease of the applied pulse duration to  $\tau = 80$  fs, the long cracks are not observed. Moreover, the black stripes seem to disappear although minor spike-like features can be observed especially at the bottom of the processed line. Overall the amount of induced defects inside the volume of the spinel has decreased significantly. We attribute this to the applied intensity of the laser pulses, which is approximately one

order of magnitude higher compare to  $\tau = 1$  ps. Therefore, the laser pulse energy is absorbed primarily in a small surface layer. Consequently, the energy deposition inside the volume of the spinel is much smaller compared to  $\tau = 1$  ps.

### 3.2 Thermal damage mechanism: Heat accumulation

For an investigation of thermal damage of the spinel due to heat accumulation, we increase the used pulse repetition rate in the order of MHz to decrease the time between subsequent laser pulses. Moreover, the spatial pulse overlap PO is varied for a coarse control of the local energy deposition. Cavities with size  $1.5 \times 0.5$  mm<sup>2</sup> are manufactured on the surface of spinel with  $N = 1$  number of scanned layers. The surface modifications for three different parameter sets are investigated by bright field microscopy. The results are shown in Figure 4.

For  $f_{rep} = 1$  MHz,  $F = 5$  J/cm<sup>2</sup> and a pulse overlap  $PO = 0.90$  (Figure 4 (a)) the surface morphology of the processed area appears homogenous and comparable to the cavities manufactured with  $f_{rep} = 200$  kHz from Figure 1. Therefore we conclude, that heat accumulation is negligible. In the next step, we increase the pulse repetition rate to  $f_{rep} = 2$  MHz and the pulse overlap to  $PO = 0.92$  (Figure 4 (b)). The morphology of the processed area appears inhomogeneous since several bright and dark features are detected. Moreover, several horizontal lines are observed which coincide with the scanning direction of the laser radiation. For a further increase of the spatial pulse overlap to  $PO = 0.98$ , the horizontal features are observed with an increased line separation distance (Figure 4 (c)). The separation distance of the observed lines is measured to approximately 25  $\mu\text{m}$  and is therefore neither corresponding to the focal spot diameter nor the separation distance between scanned lines. Consequently, the horizontal lines may cor-

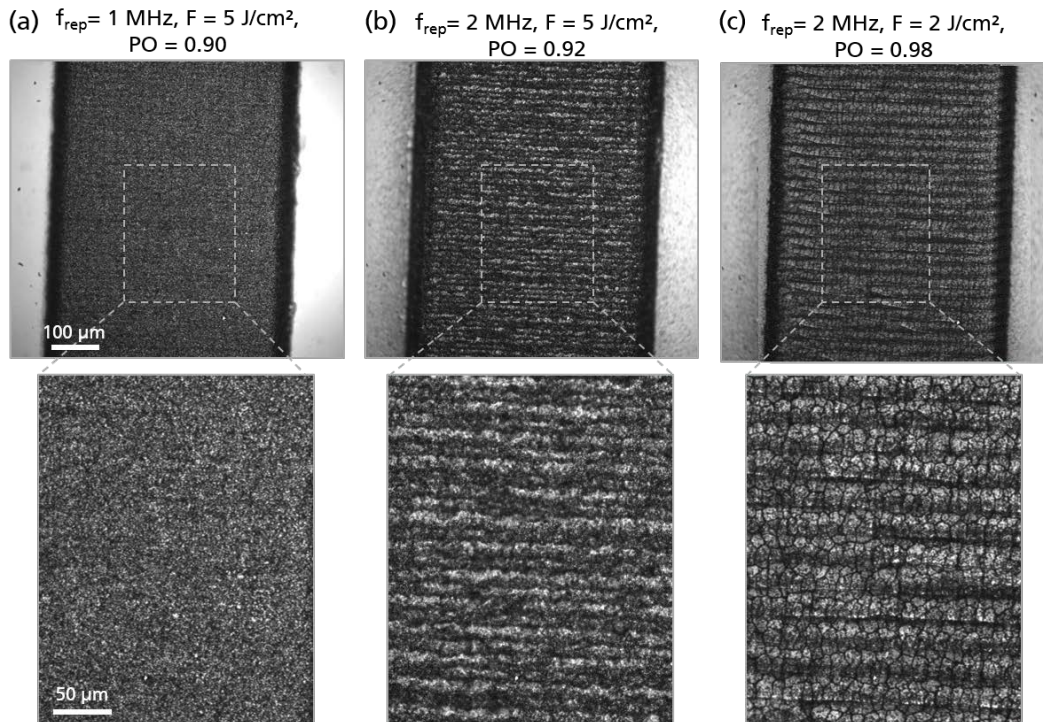


Fig. 4: Bright field microscopy of the surface of processed areas for a variation of the pulse repetition rate, fluence and spatial pulse overlap PO. The number of scanned layers  $N = 1$  is constant for all processed areas.

respond to molten rim features due to complex melting dynamics. Moreover, crust-like features are observed with sizes in the order of 10  $\mu\text{m}$ , which is much larger than the mean grain size of approximately 0.57  $\mu\text{m}$  of the spinel. Therefore we conclude, that the spatial pulse overlap PO has a major impact on the role of heat accumulation for spinel. The crust-like features indicate a self-organized modification process subsequent to the laser ablation. Due to the features of the horizontal lines and the inhomogeneous surface morphology, we conclude that heat accumulation leads to a change of local energy input and therefore a local increase of temperature exceeding the melting temperature of the spinel. Therefore, the intrinsic properties of the ceramic like the cubic crystal structure might be modified. Further investigations with a spatial resolution on an atomic scale like transmission electron microscopy may reveal structural changes on a sub-micrometer scale.

#### 4. Summary

In this study, we investigated the ultrashort pulsed laser ablation and modification process of transparent spinel  $\text{MgAl}_2\text{O}_4$  by an extensive characterization of resulting surface modifications of the processed area as well as in-volume modifications. We identify two different modification mechanisms and address regimes, for which incubation or heat accumulation are affecting the local energy deposition. Here, incubation is correlated to an electronic and accumulation to thermal damage mechanism, respectively. For incubation, the ablation takes primarily place due to vaporization. In-volume modifications are induced by the propagation of the laser pulse energy inside the glass volume due to refraction and interference caused by the surface ablation crater. For a high spatial pulse overlap, cracks in the volume occur which extend up to several 100  $\mu\text{m}$ . Moreover we have shown, that by a decrease of the applied pulse duration to  $\tau = 80$  fs, the cracks can be reduced due to the higher peak intensity of the laser pulse and the subsequent absorption in a thin surface layer only. Heat accumulation can be observed for an increase of the pulse repetition rate and the spatial pulse overlap by detection of molten rims parallel to the scanning direction of the laser radia-

tion. Furthermore, crust-like features are observed which might indicate a self-organized emerging process subsequent to the laser modification process. Additional studies on the morphological changes on an atomic scale like transmission electron microscopy can provide evidence on the underlying mechanisms leading to the observed structural changes.

#### Acknowledgments

This work was supported by the Fraunhofer Internal Programs under Grant No. MAVO 833 916.

#### References

- [1] A. Goldstein, and A. Krell: *J. Am. Ceram. Soc.*, 99, (2016) 3173.
- [2] B. C. Stuart, M. D. Feit, S. Herman, A. M. Rubenchik, B. W. Shore, and M. D. Perry: *Phys. Rev. B*, 53, (1996) 1749.
- [3] B. C. Stuart, M. D. Feit, A. M. Rubenchik, B. W. Shore, and M. D. Perry: *Phys. Rev. Lett.*, 74, (1995) 2248.
- [4] L. V. Keldysh: *Sov. Phys. JETP*, 20, (1965) 1307.
- [5] A. Vogel, J. Noack, G. Hüttman, and G. Paltauf: *Appl. Phys. B*, 81, (2005) 1015.
- [6] C. Kalupka, D. Grossmann, and M. Reininghaus: *Appl. Phys. A*, 123, (2017) 376.
- [7] M. Hermans, J. Gottmann, and F. Riedel: *J. Laser Micro/Nanoengin.*, 9, (2014) 126.
- [8] C. Kalupka, T. Holtum, and M. Reininghaus: *Proc. SPIE*, 10520, (2018) 105200G.
- [9] D. Grossmann, M. Reininghaus, C. Kalupka, M. Kumkar, and R. Poprawe: *Opt. Expr.*, 24, (2016) 23221.
- [10] M. H. Niemz: *Appl. Phys. Lett.*, 66, (1995) 1181.
- [11] A. Krell, T. Hutzler, J. Klimke, and A. Potthoff: *J. Am. Ceram. Soc.*, 93, (2010) 2656.
- [12] M. Sun, U. Eppelt, S. Russ, C. Hartmann, C. Siebert, J. Zhu, and W. Schulz: *Opt. Expr.*, 21, (2013) 7858.
- [13] J. M. Liu: *Opt. Lett.*, 7, (1982) 196.

(Received: June 25, 2018, Accepted: September 12, 2018)